Any Scalene Triangle Is the Most Chiral Triangle

by **André Rassat***[a]) and **Patrick W. Fowler***[b])

[a]) UMR CNRS 8640, Département de Chimie, Ecole Normale Supérieure, 24 rue Lhomond, F-75231 Paris CEDEX 05 (fax: (+33) 1 4432 3325, e-mail: andre.rassat@ens.fr)
[b]) School of Chemistry, University of Exeter, Stocker Road, Exeter EX4 4QD UK (fax (+44) 1392 263 434, e-mail: P.W.Fowler@exeter.ac.uk)

Dedicated to Professor *Jack D. Dunitz* on the occasion of his 80th birthday

The shape space of all possible triangles is represented by a triangular diagram, an analogue of the phase diagram for ternary mixtures. Each point of its interior corresponds to the angle set of a pair of (2D) enantiomeric physical triangles and, with appropriate conventions, to just one member of the pair. Points on median lines represent achiral triangles, those on sides represent degenerate chiral triangles, and those on vertices achiral degenerate linear triangles. A chirality index for triangles must vanish on these lines, but nowhere else within the six compartments of the diagram, and should alternate in sign between them. The archetype is the lowest A_2-symmetric eigenfunction of the *Schrödinger* equation for the particle confined to an equilateral triangular box. Within the constraints, the extrema of an acceptable function may be pushed onto any D_{3h}-symmetric hexagonal set of points in the diagram, thereby verifying a conjecture of *Dunitz* that *any* scalene triangle is the *most-chiral* triangle for some legal 2D-chirality index.

Introduction. – The importance of three-dimensional chirality in chemistry, biology, and other sciences is undisputed [1]. A well-established symmetry criterion can be used to decide whether the 'stereomodel' [2] of a molecule or other object of defined geometric structure is chiral or achiral: chiral objects possess only proper elements of symmetry, and achiral objects possess at least one improper element of symmetry. However, the notion of the *chirality content* or *degree of chirality* of a structure, and, in particular, the relationship of such a quantity with measurable molecular properties is less settled; attempts to define the relationship have inspired a vast literature (see, *e.g.*, [3] and refs. cit. therein), and the conceptual and practical aspects of 3D chirality are still subjects of active research.

Restriction of the chirality problem to two dimensions has often been used as a natural way of simplifying analysis and gaining insight [1][4][5]. In 'Flatland' [6], there is a single improper operation, a reflection in a line contained in the plane. Restriction to two dimensions also offers simplifications at a deeper level: interconversion of a chiral triangle and its enantiomer *necessarily* involves passage through an achiral intermediate structure, whilst, in all higher dimensions [7], pairs of (unlabelled) enantiomeric simplexes are 'chirally connected' in that it is possible to interconvert them by a continuous distortion pathway that does not pass through an achiral configuration.

In three-dimensional space, the two-dimensional chirality of a triangle is manifested by the fact that a chiral triangle has two distinguishable faces [1]. The special properties

of the scalene triangle have suggested to many authors [4][8–12] that this object may be a good starting point for the quantification of chirality. In particular, we might consider the question of the shape of the *most-chiral* triangle. Different answers have been proposed [4][9–16]. Several authors [10][13][14] have noted that different measures lead to different rankings, and this is exemplified by the appearance of a variety of most chiral triangles. In a reaction to this situation, *Dunitz* then '*hazarded the conjecture*' that there should exist some valid measure that will make *any* chiral triangle the *most-chiral* triangle [17]. The present note gives an explicit demonstration of the correctness of this conjecture.

Chirality Measures and Measures of Chirality. – The *degree of chirality* [18] (also called the *chirality measure* [14][19]) of an object is a real-valued continuous function (of the coordinates describing a stereomodel), which vanishes if and only if the object is achiral. This function is similarity-invariant, dimensionless and normalized to the interval [0,1], and it takes equal values for the object and its enantiomorph. Two classes of chirality measure can be distinguished, depending on whether the measure represents the difference between the object and a reference, or between the object and its enantiomorph [20].

The degree of chirality χ is a scalar. Another quantity, confusingly named the *measure of chirality* [4], is a pseudoscalar, which is also similarity-invariant, dimensionless, and normalized but is defined on the interval $[-1, +1]$ and takes *opposite* values for the object and its enantiomorph. The *degree* of chirality is then simply the absolute value of the *measure* of chirality (here called ψ), also called the *chirality index* by some authors [21], which is the term that will be used here.

When applicable, calculation of the pseudoscalar ψ has the obvious advantage over χ that it can encode simultaneously the chirality content and the identity of an enantiomer. In general, some care is needed when working with pseudoscalars in chirally connected systems if the problem of false zeroes is to be avoided [3][22][23]. However, as noted above, this *connection problem* does not arise for triangles and, so, the sign of a conveniently chosen pseudoscalar can be used as a *descriptor* to distinguish the enantiomeric forms of triangles.

A chiral triangle can be assigned a descriptor to distinguish its enantiomeric forms. If, in the spirit of the *CIP* rules for two-dimensional chiral objects [24], the three sides (or angles) are labelled as Large, Medium, and Small, the triangle is assigned a descriptor C_{LMS} (A_{LMS}) for clockwise (anticlockwise) ordering of Large, Medium, and Small. In using the original *CIP* rules, where the descriptors *Re* (*Si*) are used to distinguish the heterotopic planar faces of molecules, there is physical and chemical information that can be translated into a vertex labelling. Here, the $C_{\mathrm{LMS}}/A_{\mathrm{LMS}}$ descriptors are purely geometric, using the only information available for these mathematical objects.

Representation of the Shape Space of Triangles. – Up to similarity, a triangle ABC is specified by two independent parameters (or three parameters plus a constraint). A convenient set is that of the three internal angles, $\alpha = a\pi$, $\beta = b\pi$, $\gamma = c\pi$ where the *reduced angles* a, b, c obey $a+b+c=1$ and $a \geq 0$, $b \geq 0$, $c \geq 0$. Except in the cases of degenerate linear triangles, the normalized side lengths a_l, b_l, c_l ($a_l+b_l+c_l=1$),

automatically obeying the triangle inequalities, are recovered from the angles by $a_l = \sin\alpha/(\sin\alpha + \sin\beta + \sin\gamma)$ and permutations. Clearly, for a given physical triangle, there are six ways of labelling the vertices, say ABC, corresponding to the three even and three odd permutations of three letters.

Several representations of the two-dimensional 'shape space' of all possible triangles have been used in the chirality literature [9–11][13][15]. A convenient and symmetrical way of representing three quantities that sum to a constant is through the *triangular diagram,* introduced by *Roozeboom* [25] and used to present the thermodynamic phase properties of ternary mixtures (see, *e.g.*, [26]; a related triangular representation was used even earlier by *Lamé* in the theory of elasticity [27]). The same diagram is useful in other physical contexts, *e.g.*, for *spd* hybridization diagrams [28].

The vertices of the triangular diagram are represented here by ABC to distinguish them from those of a physical triangle ABC. In the triangular diagram, a general point P has coordinates a_P, b_P, c_P defined by distances measured parallel to the sides (with $a_P + b_P + c_P = L$, the side of the triangle ABC). If we take the coordinates of a given triangle to be the reduced angles a, b, c, and hence $L = 1$, P corresponds to the two enantiomers of one possible physical triangle, together with a specific assignment of labels ABC to its vertices.

Fig. 1 shows the coordinate system. *Isosceles* triangles are defined by points on the median lines AM_A, BM_B, CM_C, with *equilateral* triangles occurring at the centroid G. Points on the perimeter of the triangular diagram correspond to *degenerate* triangles: those on the sides are obtained as the limit of a process in which one angle tends to zero, whilst those at the vertices are obtained when two angles tend to zero. *Fig. 2* illustrates these degenerate cases, for which the normalized side lengths are not obtainable from the sine rule. In the one-zero case with $\beta = 0$, the lengths are $a_l = c_l = 1/2$, $b_l = 0$, for all α and γ; and, in the two-zero case, with $\alpha = \beta = 0$, the lengths are $a_l + b_l = c_l = 1/2$, with $0 \leq a_l \leq 1/2$.

The sixfold redundancy of labellings would lead to the appearance of any given triangle, and its enantiomer, at the six corners of a three-fold symmetric hexagon (P_1 to P_6 in *Fig. 3,a*). To remove this degeneracy, we adopt the convention that, for any triangle, the labels ABC run clockwise. With this convention, a chiral triangle, defined by a set of three reduced angles and a cyclic order LMS, is labelled by any of the three *even* permutations of ABC. If the LMS order is anticlockwise, *i.e.*, the triangle descriptor is A_{LMS}, these correspond to points P_1, P_3, P_5. The enantiomer defined by the same angles but with the opposite order of LMS and descriptor C_{LMS} corresponds to P_2, P_4, P_6 (*Fig. 3,b*). Any adjacent pair of compartments covers the shape space of physical triangles exactly once.

The triangular diagram can also be used with a parameterization of the physical triangle in terms of the lengths of the sides. If the coordinates of a given triangle are taken as the reduced sides, $a_l = l_a/2s$, $b_l = l_b/2s$, $c_l = l_c/2s$, the triangular inequality implies that the reduced coordinates can vary between 0 and ½, and the threefold-redundant shape space is now reduced to the smaller triangle $M_A M_B M_C$.

Another version of the triangular diagram has been used by *Buda*, *Auf der Heyde*, and *Mislow* [13], who identified the Cartesian coordinates x, y of *Fig. 1*, ($y = \mathrm{S}_{2a}$; $x = \mathrm{S}_{2b}$) with the components of the degenerate E distortion of the angles of an originally equilateral triangle.

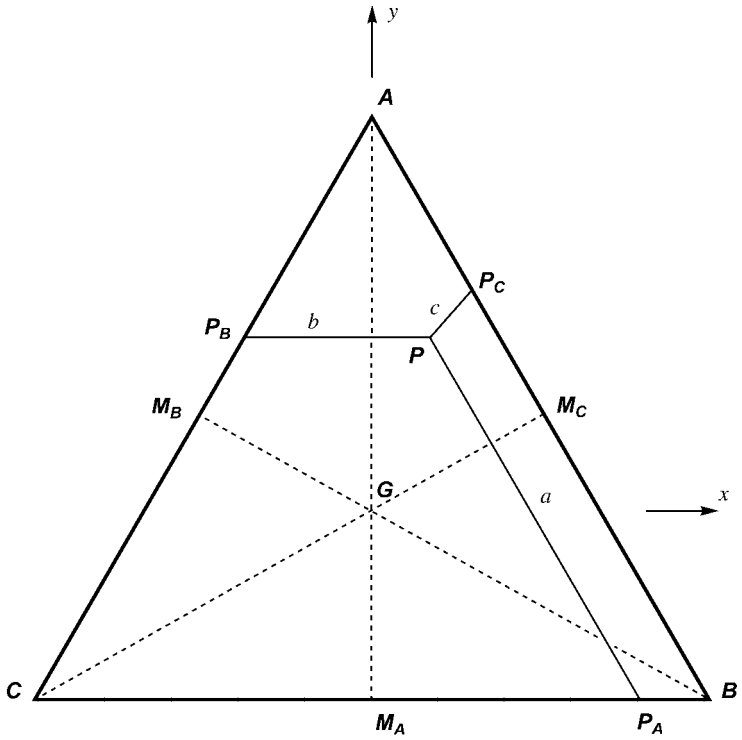

Fig. 1. *Triangular-diagram representation of the space of all possible chiral and achiral triangles.* A point *P* inside the diagram defines a physical triangle by its reduced angles *a*, *b*, *c* taken as the distances, measured parallel to the sides, to the sides of the master triangle *ABC*. As explained in the text, boundary lines correspond to achiral triangles, medians AM_A, BM_B, CM_C to isosceles triangles, *G* represents equilateral triangles, and the vertices and sides of *ABC* correspond to degenerate straight-line triangles. *Gx* and *Gy* are the axes of a Cartesian coordinate system.

Although representation of the shape space in terms of triangular diagrams is convenient, other possibilities have been proposed [10][11][15][16]. For example, *Moreau* [9] represents a triangle by inscribing it in a circumcircle of unit radius; one vertex is fixed, and the others are defined by their polar angles relative to the first.

In a construction based on lengths [13], the shape space of triangles can be represented in the upper half of the Cartesian plane (*Fig. 4*). In this representation, one side of the physical triangle (AB, of length 1) is fixed on the *x* axis and vertex C ranges over the half-plane. We note that this choice ensures a clockwise order ABC. Six regions bounded by two semicircles and the axes represent 2D-chiral triangles, with all the possible orderings of sides. Two of the regions are infinite. *Fig. 4* shows the detailed correspondence between this length-based construction and the angle-based triangular diagram. The region where $a < b < c$ corresponds to the left-hand side of a 'Gothic Arch'. The semicircular boundaries of the arch represent isosceles triangles and the equilateral triangle appears at the apex *G* of the arch. Degenerate triangles with two zero angles are situated on the *x* axis that forms the lintel of the arch and are considered

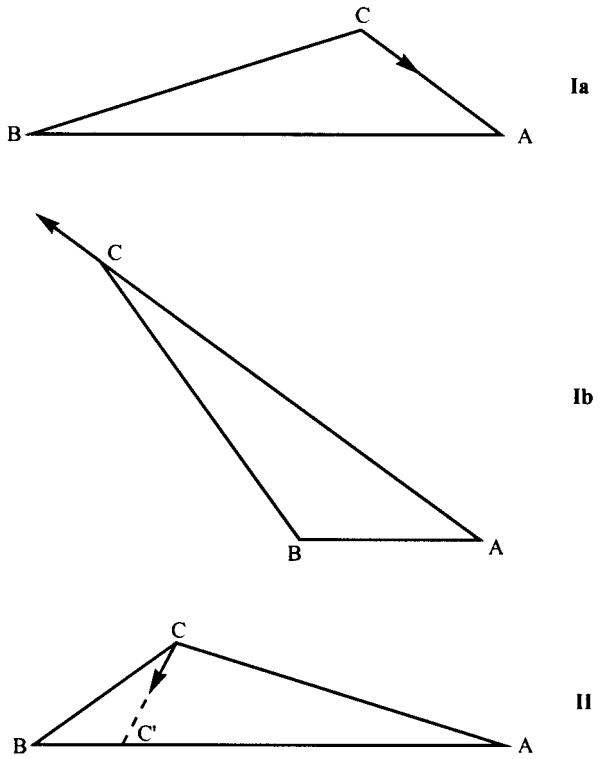

Fig. 2. *Limiting processes leading to degenerate physical triangles ABC.* **I**: Two ways to obtain degenerate triangles with a single zero angle: **Ia**: AB and α are held constant, and C is pushed into A; **Ib**: AC and α are held constant, and B is taken to infinity. In both cases, $\beta \to 0$, $\gamma \to \pi - \alpha$, leading to a point on *AC* in the triangular diagram (between *C* and M_B for $\alpha \leq \pi/2$, or between M_B and *A* for $\alpha \geq \pi/2$). **II**: A way to obtain a degenerate triangle with two zero angles: AB is held constant, and C is taken towards a point C′ on the line AB; then $\alpha \to 0$, $\beta \to 0$, $\gamma \to \pi$, $l_a \to$ BC', and $l_b \to$ C'A, so that the limiting physical triangle lies at vertex *C*.

[13] to be excluded from the shape space. We note that degenerate triangles with a single zero angle have two different representations: those called **Ia** in *Fig. 2* appear on the *x* axis at the bottom corners of the arch, those of type **Ib** are found outside the arch along the whole infinite limit of the upper half-plane.

In comparison with the gothic-arch representation, the triangular-diagram construction has the advantages that all six regions are congruent, and the copies of the enantiomers of a given physical triangle are represented simply by a set of points $P_1P_2P_3P_4P_5P_6$ related by the operations of C_{3v}. The second feature will prove useful in the discussion that follows. The topological fact that triangles are not chirally connected is expressed by the geometrical fact that, in order to pass from one compartment of the diagram to another, it is necessary to cross an achiral line (a median in the triangular diagram, a boundary curve in the gothic-arch construction).

Application to Chirality Indices. – As noted earlier, it is generally recognized that a consistent chirality index, ψ, must satisfy a number of conditions [3][13][21]. It should

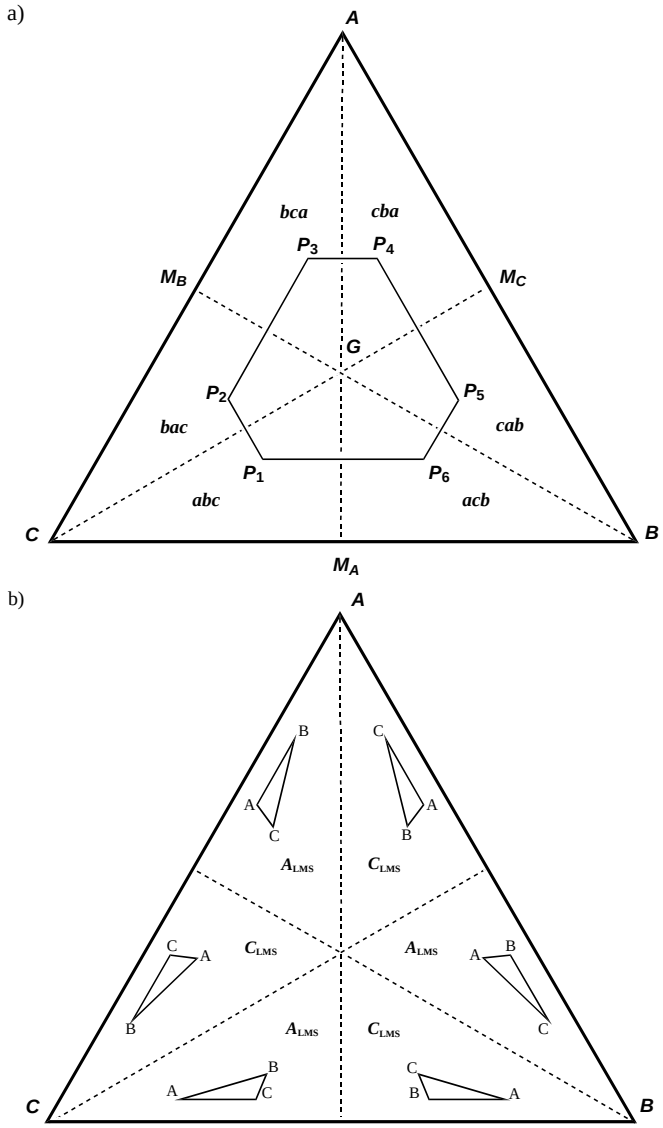

Fig. 3. *a*) *The six points,* P_1, P_2, P_3, P_4, P_5, *and* P_6, *on the triangular diagram each represent a permutation of vertex labels of a given physical triangle ABC* and its enantiomer *in the shape space defined by reduced angles* a,b,c. The six compartments are labelled by the order of the angles (*abc* denotes $a < b < c$, and so on). *b*) *With the convention that the vertex labels ABC run clockwise, alternate compartments contain the physical triangle and its enantiomer, and the 2D-chirality descriptors* C_{LMS}/A_{LMS} *can be assigned to the triangles shown.*

A) take value zero for all achiral objects in the shape space, B) should take opposite values for enantiomers, and C) should vanish *only* for the achiral objects in that space. It should also be similarity-independent, confined to the interval $-1 < \psi < +1$, and

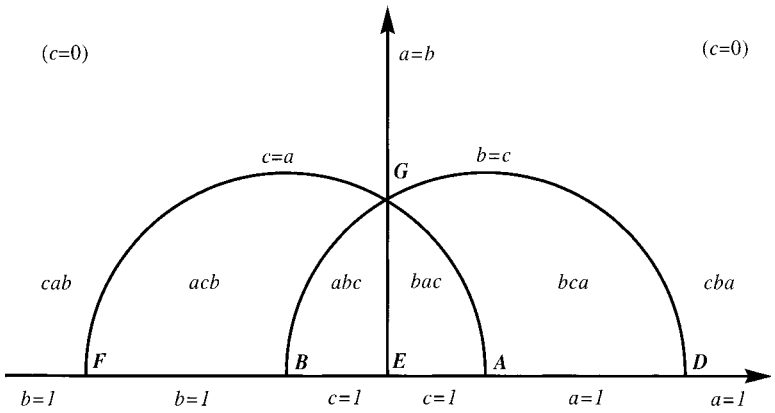

Fig. 4. *Half-plane representation of the shape space of triangles* (see Fig. 2 in [13]). The domains are labelled by the permutations of reduced angles *abc* (*abc* denotes $a < b < c$) to show the connection with the triangular diagram (*Fig. 3,a*) and relations between these reduced angles define the boundaries. ***A*** and ***B*** are vertices of the physical triangle, whilst vertex ***C*** wanders over the half-plane. The semi-circles ***AGF*** and ***BGD*** correspond to the medians BM_B and AM_A, and the positive half of the vertical axis ***EG***... to the median CM_C, with M_C at infinity. All points on the line segment ***AB*** correspond to vertex *C* of the triangular diagram, and those on the semi-infinite axes ***AD***... and ***BF***... to vertices *A* and *B*, respectively. Points ***A*** and ***B*** correspond to the sides *AC* and *BC* of the triangular diagram, whilst the set of points at infinity in the upper half-plane (denoted by ($c = 0$)) corresponds to the side *AB*. The special point ***G*** corresponds to the equilateral triangle (*G* in *Fig. 1*).

should be a continuous function of shape. We may add D) the function should have a single maximum in the shape space. A desirable property, already implicit in the way that we construct the triangular diagram, is E) that ψ should be independent of vertex labelling.

The triangular diagram gives a straightforward translation of this set of conditions, to be obeyed by any function $\psi\ (a,b,c)$ that is to be a candidate for a chirality index:

Condition A deals with the set of achiral triangles for which the function should vanish, which includes isosceles, equilateral, and degenerate triangles. Hence, ψ must have nodes along *all six* special lines of the triangular diagram, *i.e.*, along the medians and sides

$$\begin{gathered}\psi\ (\alpha,\ \alpha,\ 1-2\alpha) = \psi\ (\alpha,\ 1-2\alpha,\ \alpha) = \psi\ (1-2\alpha,\ \alpha,\ \alpha) = 0,\\ \psi\ (\alpha,\ 1-\alpha,\ 0) = \psi\ (\alpha,\ 0,\ 1-\alpha) = \psi\ (0,\ \alpha,\ 1-\alpha) = 0.\end{gathered} \tag{1}$$

Condition B is a requirement that ψ should be of opposite sign in alternate compartments of *ABC:*

$$\psi\ (\alpha,\beta,\gamma) = \psi\ (\beta,\gamma,\alpha) = \psi\ (\gamma,\alpha,\beta) = -\psi\ (\alpha,\gamma,\beta) = -\psi\ (\beta,\alpha,\gamma) = -\psi\ (\gamma,\beta,\alpha). \tag{2}$$

Thus, in terms of a C_{3v} point-group description of the triangular diagram, the function ψ must belong to the antisymmetric irreducible representation A_2 of that group. Notice that multiplication of ψ by any totally symmetric (A_1) function $S(a,b,c)$ of the angles

provides a new A_2 function, which will also be a legitimate chirality index if this multiplication does not introduce any new nodes, *i.e.*, false zeroes.

Condition C is, thus, obeyed by making suitable choices of ψ and *S*. We also impose the condition that this ψ function will have a single extremum in each compartment (*i.e.*, condition D), giving maxima and minima on alternate vertices of a hexagon $P_1P_2P_3P_4P_5P_6$.

Various functions can easily be derived to fit these restrictions. One obvious candidate is the lowest A_2 eigenfunction of the *Schrödinger* equation for the particle confined to an equilateral triangular box [29] (or of an equivalent vibrational problem [27]),

$$\begin{aligned}\psi_P = &\cos[2\pi(2a-b)] + \cos[2\pi(2b-c)] + \cos[2\pi(2c-a)] \\ &- \cos[2\pi(2b-a)] - \cos[2\pi(2c-b)] - \cos[2\pi(2a-c)],\end{aligned} \tag{3}$$

which, by construction, has exactly the required nodal behaviour. Higher A_2 solutions of the particle-in-an-equilateral-triangular-box problem have extra nodes and would, therefore, bring in false zeroes, ruling them out as usable in the context of chirality.

The three-term triangular analogue [13] of the tetrahedral *Guye* function [30],

$$G(a,b,c) = (a-b)(b-c)(c-a), \tag{4}$$

which is obtained from the 3×3 *Vandermonde* determinant or by projection of a function such as ab^2, has the correct A_2 symmetry behaviour, but it vanishes only on the median lines and not on the sides of the triangular diagram. Multiplication by the A_1 function *abc* yields a *Guye*-like chirality index defined by a product of six linear factors, each vanishing along one special line of *ABC:*

$$\psi_G = abc(a-b)(b-c)(c-a). \tag{5}$$

A third function is the sine modification of the three-term *Guye* function proposed by *Dunitz* [17]:

$$\psi_D = (\sin\pi a - \sin\pi b)(\sin\pi b - \sin\pi c)(\sin\pi c - \sin\pi a). \tag{6}$$

It has the proper nodal behaviour, as each factor ensures satisfaction of two nodal conditions, since $\sin u = \sin v$ implies $u = v$ or $u = \pi - v$, and there is no need for further multiplication by *abc* or the like.

The functions ψ_D, ψ_P, and ψ_G can be normalized to the range $[-1, +1]$ and made positive in a selected region, *e.g.*, where $a < b < c$. They already satisfy the requirement of a single maximum/minimum per compartment of *ABC*.

Some functions are less well-suited for use as chirality indices. *Buda et al*. obtained a normalized and similarity-independent chirality index [8][13], which can be written in our notation

$$\psi\ (\text{sides}) = (1 - l_b/l_a)(1 - l_c/l_b)(1 - l_a/l_c) \tag{7}$$

by multiplying the *Guye* function for sides, $G\ (l_a, l_b, l_c)$, by the symmetric function $(l_a l_b l_c)^{-1}$. Although the multiplying term becomes infinite when a side shrinks to zero length, the index does not diverge, as the value of AB is fixed. This function would not be usable as a general chirality index in situations where side lengths are varying under a different similarity-related constraint. Furthermore, contrary to our interpretation of (A), the restriction that a chirality index should vanish for all achiral objects is not satisfied by ψ(sides) for degenerate triangles. For instance, for the limiting degenerate triangles of *Fig. 2*, in case **Ia**, $\psi(\text{sides}) = -\cos\alpha$, and in case **II**, $\psi(\text{sides}) = (1 - 2\,|\,\text{BC}\,|\,)$ (or $(1 + 4l_a)$ in our convention).

Similarly, although it has the correct A_2 symmetry, the corresponding angle function

$$\psi\ (\text{angles}) = (1 - b/a)(1 - c/b)(1 - a/c) \tag{8}$$

cannot be used as a general chirality index, as it becomes infinite or undefined on the boundaries of the triangular diagram.

The Most-Chiral Triangle. – The *Table* lists the most-chiral triangles obtained with the three functions ψ_D, ψ_P, and ψ_G, and compares them with previously published results. As *Fig. 5* shows, most of the extremal triangles occupy the central region of each compartment of the triangular diagram. This clustering of extrema is not a necessary property of ψ functions. We have seen that multiplication of a chirality index ψ by a conveniently chosen A_1 function affords a new legitimate chirality index as acceptable as the original. If we use a family of such symmetric functions depending on one

Table. *Predictions for the Most Chiral Triangle According to Different Chirality-Index Functions.* α, β, and γ are the three angles of the triangle; a value in square brackets indicates a limit [13].

Source Ref.	α	β	γ
[4]	[0]	[0]	[180]
[8, 13]	[0]	[60]	[120]
[13]	[0]	[90]	[90]
[10]	12.2	37.4	130.4
This work, ψ_G	14.0	49.6	116.4
[17], ψ_D	15.5	52.3	111.9
[10]	15.7	35.7	128.6
[14]	16.4	37.7	125.9
[15]	16.8	37.8	125.4
[16]	16.9	37.5	125.3
[11]	17.2	38.0	124.8
[14]	17.6	40.9	121.5
[8]	18.8	71.2	90.0
[14]	21.0	43.7	115.3
[14]	21.2	43.5	115.4
This work, ψ_P	21.3	57.2	101.5
[13]	21.5	44.2	114.3
[14]	24.3	48.6	107.1
[16]	28.8	50.87	100.4
[9]	31.5	57.0	91.5
[8]	37.5	52.5	90.0

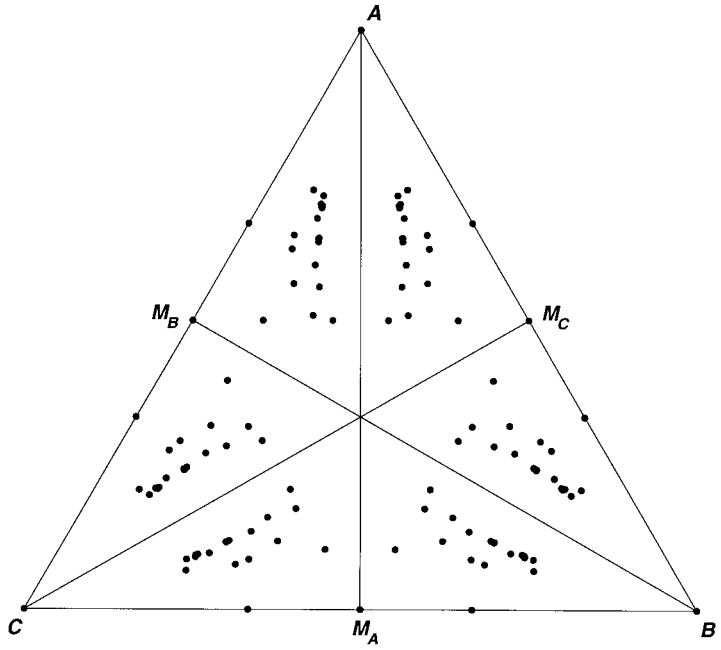

Fig. 5. *Predictions for the most-chiral triangle according to the different chirality-index functions listed in the* Table

continuous parameter, the extrema will define a continuous curve in the triangular diagram. *Fig. 6,a* demonstrates the effects of applying such 'pushing functions' to the modified *Guye* function (*Eqn. 5*). The functions plotted are $S_k(a, b, c)\ \psi_G$ where for $p > 0$

$$\begin{aligned} S_1 &= (a^p + b^p + c^p), \\ S_2 &= (a^p + b^p + c^p)^{-1}, \\ S_3 &= 4^p\ (a^p b^p + b^p c^p + c^p a^p). \end{aligned} \tag{9}$$

Transformations S_1 and S_2 push the extrema to the vertices and centroid of the ABC diagram, respectively. Under transformation S_3, the extrema follow a more complicated path before moving off to the edge-midpoints of ABC. The extrema can be pushed arbitrarily close to the vertices of the six regions by increasing the exponent parameter p. Very similar results are obtained from the equivalent transformations of other A_2 starting functions.

Two-parameter families that cover the entire shape space are also easily devised. For example, multiplication of ψ_G by the totally symmetric combination

$$\begin{aligned} F_\lambda = &\exp\left[-\lambda\, f(a,b,c)\right] + \exp\left[-\lambda\, f(b,c,a)\right] + \exp\left[-\lambda\, f(c,a,b)\right] \\ &+ \exp\left[-\lambda\, f(c,b,a)\right] + \exp\left[-\lambda\, f(a,c,b)\right] + \exp\left[-\lambda\, f(b,a,c)\right], \end{aligned} \tag{10}$$

a)

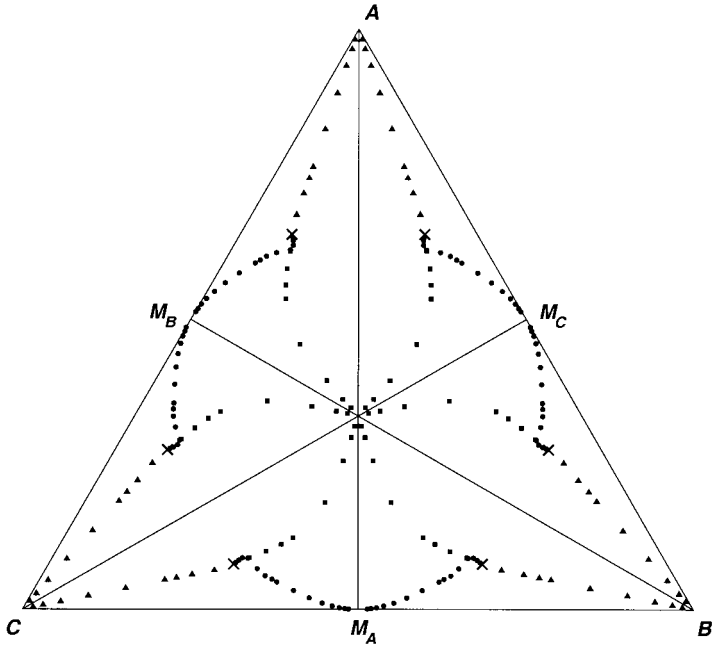

b)

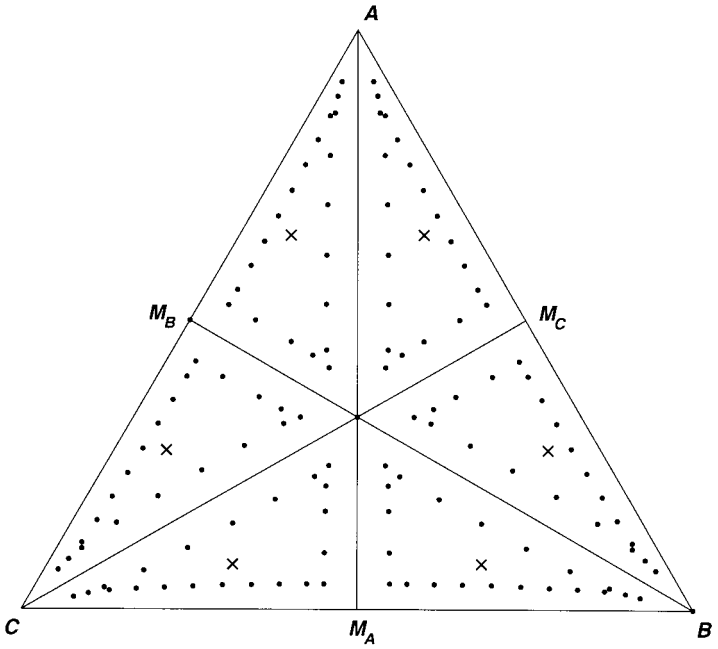

gives such a family, where

$$f(a,b,c) = (a-u)^2 + (b-v)^2 + (c-w)^2, \tag{11}$$

u,v,w are fixed parameters, $(u+v+w=1)$ and λ is a positive exponent. The product $F_\lambda\,\psi_G$ is a function whose extrema lie in the vicinity of the target point $a=u, b=v, c=w$ and its five images. The extrema can be pushed arbitrarily close to the target points by increasing λ.

Fig. 6,b, shows the area covered in the triangular diagram by the extrema for $\lambda = 100$. When the target points are chosen on the edge of the compartment, the extra extremum travels over a 'triangular' region with curved sides. As λ is increased, the boundaries of this region can be made to approach arbitrarily closely to the walls of the each compartment. In the limit $\lambda \to \infty$, F_λ becomes a combination of delta functions, yielding in the triangular diagram a crown of spikes, three pointing up and three pointing down, and the extrema are then exactly at the points corresponding to the target parameters u,v,w and permutations.

This simple argument thus demonstrates the correctness of *Dunitz*'s conjecture. It is indeed the case that, with an appropriate choice of chirality index, any scalene triangle can be found to be the most-chiral triangle.

REFERENCES

[1] V. Prelog, *Science* **1976**, *193*, 17.
[2] V. Prelog, G. Helmchen, *Angew. Chem.* **1982**, *94*, 614; *Angew. Chem., Int. Ed.* **1982**, *21*, 567.
[3] N. Weinberg, K. Mislow, *Can. J. Chem.* **2000**, *78*, 41.
[4] A. B. Buda, K. Mislow, *THEOCHEM-J. Mol. Struct.* **1991**, *78*, 1.
[5] C. E. Wintner, *J. Chem. Educ.* **1983**, *60*, 550.
[6] E. A. Abbott, 'Flatland, A Romance of Many Dimensions', Basil Blackwell, Oxford, 1978.
[7] N. Weinberg, K. Mislow, *Theor. Chim. Acta* **1997**, *95*, 63.
[8] A. B. Buda, T. Auf der Heyde, K. Mislow, *J. Math. Chem.* **1991**, *6*, 243.
[9] G. Moreau, *J. Chem. Inf. Comput. Sci.* **1997**, *37*, 929.
[10] R. Chauvin, *J. Math. Chem.* **1996**, *19*, 147.

← Fig. 6. *Predictions for the most-chiral triangle. a*) Predictions according to the one-parameter families of chirality-index functions based on the modified *Guye* function ψ_G multiplied by the pushing functions S_1 to S_3. The crosses mark the extrema for ψ_G itself. The set of filled triangles leading from the cross to a vertex of the diagram mark the extrema for the function $S_1\,\psi_G$ with $p = 2, 3, 4, 5, 10, 20, 40, 80, 160$. The set of filled squares leading from the cross to the centre of the diagram mark the extrema for the function $S_2\,\psi_G$ with $p = 2, 3, 4, 5, 10, 20, 40, 80$. The set of filled circles leading from the cross to the edge-midpoints of the diagram mark the extrema for the function $S_3\,\psi_G$ with $p = 0.1, 0.25, 0.5, 1, 2, 3, 4, 5, 10, 20, 40, 80, 160, 320, 640$. *b*) *Predictions according to a two-parameter family of chirality-index functions based on the modified* Guye *function* ψ_G *with the exponential pushing function* F_λ. The crosses mark the extrema for ψ_G. The dotted region shows the extrema of $F_\lambda\,\psi_G$ with fixed exponent $\lambda = 100$, when the target parameters u,v,w are moved along edge lines in the shape space. For $w = 0$ and $0 < v = 1 - u < 0.5$, the extrema track the outer edge of each compartment. For $0 < u = v = (1-w)/2 < 0.5$, the extrema track one median line in from near a vertex towards the central point, and back towards an edge midpoint. The perimeter of the compartment can be approximated arbitrarily closely by increasing the exponent λ. Variation of λ, u, v, and w thus allows all points in the compartment to be reached and to be predicted as the most-chiral triangle by some legitimate chirality index.

[11] H. Zabrodsky, D. Avnir, *J. Am. Chem. Soc.* **1995**, *117*, 462.
[12] T. Auf der Heyde, A. B. Buda, K. Mislow, *J. Math. Chem.* **1991**, *6*, 255.
[13] A. B. Buda, T. Auf der Heyde, K. Mislow, *Angew. Chem.* **1992**, *104*, 1012; *Angew. Chem., Int. Ed.* **1992**, *31*, 989.
[14] N. Weinberg, K. Mislow, *J. Math. Chem.* **1993**, *14*, 427.
[15] Z. Zimpel, *J. Math. Chem.* **1993**, *14*, 451
[16] M. Petitjean, *J. Math. Chem.* **1997**, *22*, 185.
[17] J. Dunitz, personal communication to A.R., 11 October 2000
[18] A. B. Buda, K. Mislow, *J. Am. Chem. Soc.* **1992**, *114*, 6006.
[19] D. Avnir, A. Y. Meyer, *THEOCHEM-J. Mol. Struct.* **1991**, *72*, 211.
[20] N. Weinberg, K. Mislow, *J. Math. Chem.* **1995**, *17*, 35.
[21] M. A. Osipov, B. T. Pickup, D. A. Dunmur, *Mol. Phys.* **1995**, *84*, 1193.
[22] A. Rassat, I. Làszló, P. W. Fowler, *Chem.–Eur. J.* **2003**, *9*, 644.
[23] A. B. Harris, R. D. Kamien, T. C. Lubensky, *Rev. Mod. Phys.* **1999**, *71*, 1745.
[24] R. S. Cahn, C. K. Ingold, V. Prelog, *Experientia* **1956**, *12*, 81; b) R. S. Cahn, C. K. Ingold, V. Prelog, *Angew. Chem.* **1966**, *78*, 413; *Angew. Chem., Int. Ed.* **1966**, *5*, 385; c) V. Prelog, G. Helmchen, *Angew. Chem.* **1982**, *94*, 614; *Angew. Chem., Int. Ed.* **1982**, *21*, 567.
[25] H. W. B. Roozeboom, *Z. Phys. Chem.* **1894**, *15*, 145.
[26] P. W. Atkins, 'Physical Chemistry', 5th edn., Oxford University Press, Oxford, 1994, p. 259; J. Jacques, A. Collet, S. H. Wilen, 'Enantiomers, Racemates, and Resolutions', John Wiley & Sons, New York, 1981, p. 170; A. Findlay, 'The Phase Rule and its Applications', Longmans, Green and Co. London, 5th Edition, 1923, p 191 (where a triangular representation introduced by Gibbs in 1876 is also presented).
[27] M. G. Lamé, 'Leçons sur la Théorie Mathématique de l'Élasticité des Corps Solides', Bachelier, Paris, 1852, p. 131.
[28] W. J. Moore, 'Physical Chemistry', 5th edn., Longman, London, 1972, p. 710.
[29] a) J. K. Bhattacharjee, K. Banerjee, *J. Phys. A-Math. Gen.* **1987**, *20*, L759; b) W. K. Li, S. M. Blinder, *J. Chem. Educ.* **1987**, *64*, 130; c) W. K. Li, S. M. Blinder, *J. Math. Phys.* **1985**, *26*, 2784.
[30] P. A. Guye, *C. R. Hebd. Séances Acad. Sci.* **1893**, *116*, 1451, 1454 (*cf.* note 1 p. 1452).

Received April 1, 2003